

Design and Development of Hybrid Microgrid Control System for Renewable Energy Generation

Faisal Abbas Ali Ahmad¹, Adel H Alshatti²

^{1,2}Department of Electrical Engineering

Shuwaikh Institute, The Public Authority for Applied Education and Training (PAAET)

Kuwait

ABSTRACT

Renewable energy sources are widely acknowledged as the optimal substitutes for conventional energy outlets globally. Countries are endowed with diverse renewable resources, including solar, wind, biomass, hydro, and tidal energy. Despite this abundance, there exists a substantial disparity between the demand and supply of electrical energy, with numerous regions still facing insufficient access to power. The integration of various renewable energy sources in remote and isolated locations forms a Microgrid (MG), catering adequately to local energy requirements. These microgrids have the capability to function seamlessly alongside conventional grids. Hybrid MG system, incorporating Photovoltaic (PV) with battery storage and a Wind Turbine (WT), emerges as a practical solution for electrifying remote areas in islanded mode. The WT's installed capacity is chosen to meet critical load requirements during periods of non-availability of renewable sources. The battery's capacity is selected to cover the transition period between renewable sources or as a backup source, ensuring cost-effectiveness over WTs. The application of Adaptive Particle Swarm Optimization (APSO) has demonstrated favorable outcomes compared to existing PSO algorithms, enhancing control efficiency. In a grid-connected MG system, the integration of distributed PV generation has notably improved the voltage profile, reducing overall losses. Consequently, the presented MG systems provide both technically and economically viable solutions for ensuring continuous electricity supply in isolated and grid-connected systems. This approach not only mitigates pollution but also allows for the possibility of capacity addition, fostering sustainable growth in these regions.

Keywords: Grid Control, Micro grid, Power Generation, Power Distribution, Optimization, Renewable Energy.

I. INTRODUCTION

Global energy consumption is on the rise, and the reliance on fossil fuels to meet this demand is depleting these resources rapidly due to their finite nature. The utilization of fossil fuels not only contributes to environmental issues such as pollution and global warming but also faces limitations due to safety concerns and growing opposition from local communities, as observed in the case of nuclear energy. Given the undesirable release of contaminants and the exhaustible nature of fossil fuels, there is a need to explore alternatives that are both renewable and pollution-free. These renewable energy sources, recognized for their inexhaustible nature, offer numerous advantages over traditional energy sources [1]. As concerns for Earth's well-being intensify and energy demands continue to soar, the popularity of these renewable resources has surged. A self-sustaining circular process ensures that the resource base and supply potential remain intact despite continuous utilization.

Microgrid (MG) functions as a hybrid system, integrating one or more renewable energy sources with conventional sources to fulfil local energy demands. It is characterized as an electrical power network with at least one distributed energy source supplying various loads and operating in grid [2]. The MG presents advantages such as reduced losses, enhanced power reliability, and decreased reliance on the local grid. Various decentralized renewable energy conversion systems, including solar Photovoltaic (PV) modules, Wind Turbines (WT) and geothermal generators, are connected to a common electrical node known as a common bus, contributing to further loss reduction within the MG [3]. For system reliability, Diesel Generators (DGs) and heat and electricity storage systems are

integrated into the MG. Typically, DGs and batteries supply power when renewable sources like PV, WT, or micro-hydro are unavailable or insufficient compared to the power demand [4]. The dependence on environmental conditions poses a significant challenge for a single renewable energy source, prompting the adoption of hybrid systems involving renewables, batteries, and DGs to ensure uninterrupted power supply to connected loads [5].

The main challenge in a microgrid lies in controlling voltage and frequency amidst power demand variations. Therefore, the implementation of a Virtual Switch Interface (VSI) controller is crucial for managing these parameters under varying loads [6]. In recent decades, conventional control strategies have been employed to enhance the reliability of renewable energy sources. Artificial Intelligence (AI) techniques have emerged as effective tools for improving reliability and performance compared to traditional methods.

2. LITERATURE SURVEY

The pursuit of creating novel and effective systems has resulted in the emergence of various inventions applied across different technological domains. Researchers have dedicated significant efforts to record these innovations through research papers, patents, books, reports, and technical notes. These databases serve as the foundation for researchers embarking on further investigations in their respective fields. This section focuses on an extensive literature review conducted to examine past studies, both closely and loosely related, in the chosen research areas.

Jewell *et al.* [7] outlined an approach for assessing the capacity needs of a hybrid system. Their analysis focused on a hybrid configuration incorporating Photovoltaic (PV) with a storage battery and a wind system. The discussion highlighted the growing popularity of renewable energy resources, driven by escalating conventional fuel costs and their eco-friendly attributes. While standalone renewable systems faced reliability issues due to their dependency on weather conditions for power generation, the authors emphasized the necessity for a hybrid system to generate sufficient power to meet the load requirements and proposed a simulation method for evaluating the adequacy of power capacity. Jiang *et al.* [8] conducted an assessment of the viability of grid-connected PV generation in Singapore. The discussion highlighted that solar energy has become the fastest-growing renewable energy source, thanks to technological advancements and reduced capital costs. The conventional efficiency of each solar module type was determined, leading to the conclusion that monocrystalline modules exhibited the highest efficiency, followed by polycrystalline modules, and thin-film modules with the lowest efficiency.

Lau *et al.* [9] investigated the dependability of power provision and its integration into the proposed system. The design ensured that during regular operation, PV and wind sources supplied power to the load. Kanchev *et al.* [10] introduced a framework tailored for MG examination. This system handled centralized management at the microgrid's generation site, while the other managed local power fluctuations. A communication network was devised to facilitate data transfer between these two systems. By referring power generation and forecasting local variables, the proposed energy management system effectively regulated power flow from various sources.

Jian *et al.* [11] investigated a self-contained renewable energy system, simulating the actual configuration of an island and subsequently suggesting an optimal capacity arrangement. In isolated island renewable power systems, the crucial factors influencing system performance were identified as wind speed and the proportion of installed capacity for wind turbines. These findings have the potential to provide guidance for future research endeavors and engineering designs. Raju *et al.* [12] examined the inverter control mechanism for integrating a distributed generation system with the grid. This approach was developed and assessed utilizing MATLAB/Simulink. Additionally, the controller had the capability to fulfil the reactive power needs of the load, eliminating the need for additional power conditioning equipment. The design of the controller facilitated bidirectional power transfer with the feeder. Badwawi *et al.* [13] suggested the adoption of a Fuzzy Logic Controller (FLC) to manage the power distribution within an islanded AC microgrid (MG). Their proposed control system integrated FLC without necessitating communication links between the different MG units. However, it's essential to note that the primary limitations of fuzzy controllers lie in their dimensionality and tuning.

This research encompasses the prospective applications of hybrid systems in remote areas, specifically focusing on distant regions. This involves the collection of comprehensive data on domestic electrical load profiles from these

remote locations. Subsequently, a dedicated effort is made to design, analyze, and efficiently manage a microgrid through the implementation of an improved technique. The study extends its scope to assess the feasibility of introducing grid-connected distributed PV generation. To gain deeper insights and ensure optimal functionality, simulations are conducted for the meticulous design of MG. This comprehensive approach aims to enhance the understanding and implementation of sustainable energy solutions in geographically challenging and remote areas.

3. METHODOLOGY

The MG under examination is characterized as a hybrid system, including a PV system, WT, and a battery bank, all interconnected with the grid as depicted in Fig. 1. The management of power supplied to the connected load follows a prioritized approach, favoring renewable sources, the battery bank, and the local grid in that order [14]. The battery is primarily employed during the transition in exclusively off-grid scenarios. Any surplus power available is directed towards charging the batteries when possible. To prevent overcharging of batteries from renewable sources in off-grid mode, a dump load is integrated into the MG.

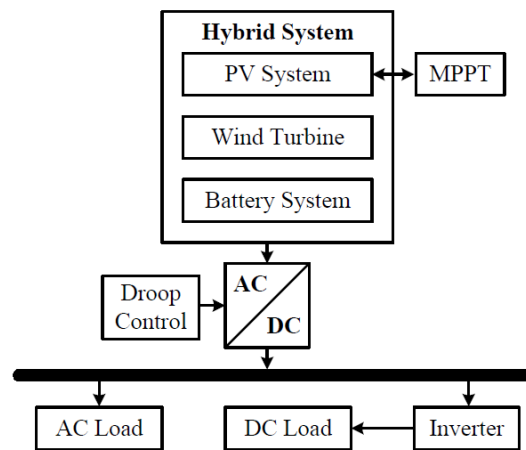


Fig. 1: Proposed Microgrid Configuration.

To regulate power in the proposed MG system, an approach based on Adaptive Particle Swarm Optimization (APSO) is explored. The electrical power required by the grid serves as the reference input. In enhancing the droop control for the control strategy analysis, the suggested technique is integrated. This control strategy effectively manages the power flows between the energy sources and the MG. In scenarios where the generated power fall behind the load demand, the battery fulfills the requirements within specified operational limits [15]. The controller outlined in this paper is employed to uphold voltage regulation and meet reactive and active demand in accordance with varying loads.

a. Hybrid System

The proposed hybrid system consists of three components: wind turbine, PV system, and a battery. Its purpose is to sustain a consistent voltage at the common bus, adapting to variable load and weather conditions. The power output of the WT is computed using Equation 1.

$$P_w(t) = \begin{cases} 0 & \text{if } W(t) \leq W_l \\ iW^3(t) - jP_r & \text{if } W_l < W(t) \leq W_r \\ P_r & \text{if } W_r \leq W(t) \leq W_0 \\ 0 & \text{if } W(t) \geq W_0 \end{cases} \quad (1)$$

$$i = \frac{P_r}{W_r^3 - W_l^3} \quad (2)$$

$$j = \frac{W_l^3}{W_r^3 - W_l^3} \quad (3)$$

In this context, the variables are defined as follows: W represents the wind speed in m/s, W_1 is the cut-in speed, W_R is the rated wind speed, and W_0 is the cut-off speed. The rated power P_r is expressed as a function of the swept area of the wind turbine generator blades (A_{WT}), the power coefficient (C_p), the reducer efficiency (η_r), reducer voltage (V_r), air density (ρ_r), and the wind turbine efficiency (η_{wt}).

$$P_r = \frac{A_{WT} C_p \rho_a \eta_r \eta_{WT} V_r^3}{2} \quad (4)$$

Solar energy is transformed into electrical power through PV panes. The Maximum Power Point Tracking (MPPT) algorithm supplies the reference voltage necessary to operate the PV system at its maximum power capacity. The equation representing the power output from PV panels at a specific time is expressed in Equation 5. Here R_t is the resistance, η_{PV} is the efficiency of PV system and A_{PV} is the area of the PV system.

$$P_{PV}(t) = R_t \eta_{PV} A_{PV} \quad (5)$$

Based on the time spent and productivity calculations, the State of Charge (SOC) of battery, is determined. If the generated energy surpasses the demand, the battery goes to charging state; conversely, if the generated energy falls short of the demand, the battery goes to discharging state. The amount of charge in the battery t is calculated using Equation 6.

$$B_s(t) = B_s(t-1) - \frac{\left(\frac{E_D(t)}{\eta_{inv}} - E_G(t) \right)}{\eta_{bf}} \quad (6)$$

Where, $B_s(t)$ represents energy demand at t , $E_D(t)$ represents the energy demand at t , $E_G(t)$ is the generated energy at time t , η_{inv} is the efficiency of the inverter and η_{bf} denotes the discharging efficiency.

b. Grid Converter

The grid-side converter is employed to supply power at a consistent voltage. The generated power is managed through the in-phase current component, which is proportionate to the load demand. In Fig. 2, a control mechanism for a grid-connected inverter is depicted, where the droop controller facilitates power output by generating an error signal from measured and command signals. Enhancing power quality at the Point of Common Coupling (PCC) is achievable through the effective design of the controller and filter. For MPPT, the voltage and currents of the PV array are scrutinized [16]. The controller computes the charging or discharging current of the battery for MPPT and, consequently, determines the maximum power that can be delivered to the grid. The MPPT controller design encompasses various parameters, as discussed below.

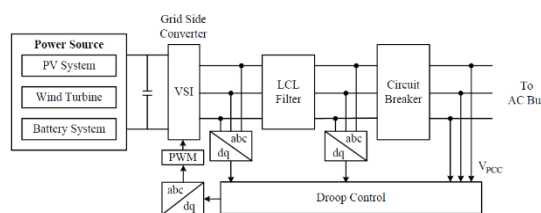


Fig. 2: Inverter Control for Grid.

C. MG Control Model

The control model of the MG is examined concerning the AC voltage and current of the battery inverter system. The inverter is responsible for supplying the output current and load voltage to the droop-controlled MG. Measurements of grid voltage and current allow the calculation of active and reactive power. The droop control unit incorporates Adaptive Particle Swarm Optimization (APSO) for optimization and inverter control. The APSO algorithm is employed to derive inverter gate pulses, which are then applied to the solar PV inverter and battery inverter, resulting in the corresponding outputs.

The initial optimizer exploits two points, A_1 and A_2 which are created within $[0, 1]$. The superior point is assigned as A_1 , while the remaining becomes A_2 . A_1 plays a role in the exploitation phase, focusing on exploiting known regions, while A_2 emphasizes exploration behaviors, probing unfamiliar areas. These points serve as focal points to explore the hypersphere measurements within the solution space, indicated by radii B_1 and B_2 , respectively.

Notably, these spans exhibit self-adaptive characteristics, with B_1 inclined to occasional decrease and B_2 to increase. The initial optimizer encompasses two essential phases: the splitting phase and archive phase. In one-way splitting, 2D copies of A are retained, and one variable of each in Y is adjusted using Equations 7 and 8. During the splitting step, entire factors of A in Y undergo adjustment using Equation 9.

$$Y_j = Y^j + aB \tag{7}$$

$$Y_{D+j} = Y^j - aB, \quad j = 1, 2, 3, \dots, D \tag{8}$$

$$Y_k^j = Y^j + \frac{aB}{\sqrt{2}} \tag{9}$$

Where, $k = 1, 2, 3, \dots, 2D$ and $j = 1, 2, 3, \dots, D$. Here, M matrix is built by selecting 2D specific numerals in the range $[0, 2^{D-1}]$.

PSO employs a collective of particles that traverse the objective domain to identify the most fit particle. During this process, all search agents temporarily follow the trajectory of the best solution. The PSO can be mathematically represented using Equation 10.

$$v_i^{t+1} = \omega v_i^t + c_1 \phi_1 (p_i - x_i^t) + c_2 \phi_2 (p_g - x_i^t) \tag{10}$$

$$x_i^{t+1} = x_i^t + v_i^{t+1} \tag{11}$$

Where, v_i^{t+1} represent velocity of, w is the weight, c_j is the acceleration, ϕ_1 and ϕ_2 comes in the range $[0,1]$, x_i^t is the current agent location, p_i is the optimum solution.

The first stage of PSO involves initiating the optimizer to generate optimal results. Subsequently, the outcomes of the optimizer serve as a starting point for PSO. Another distinction lies in the fact that PSO explores the landscape of the target issue, after which the optimizer is activated again to enhance the local search capabilities of PSO. In this proposed approach, both the optimizer and PSO are employed to address the load-sharing problem, with a primary focus on adjusting the droop control parameters. The fitness problem $f(x)$ for the hybrid system is represented by Equation 12.

$$f(x) = \{P_w(t), P_{pv}(t), B_s(t), mp, mq\} \tag{12}$$

In this context, mp and mq represent the droop parameters for active power and reactive power, respectively. $P_w(t)$ denotes the power of wind turbine, $P_{pv}(t)$ express the power of PV system and $B_s(t)$ is the power of the battery system. The primary aim is to regulate the power flow within the hybrid systems and the MG. Following this, the conventional PSO method proceeds to explore the landscape of the target problem. Subsequently, the initial optimizer is reactivated to enhance the local search capabilities of the PSO. This process continues until the conclusion of the final iteration. The proposed APSO combines the key advantages of both the initial optimizer and PSO.

4. RESULTS AND DISCUSSIONS

The MG controller is designed in MATLAB/Simulink, and analyzed in both off-grid and on-grid modes, considering varying loads and renewable sources. Table 1 delivers a summary of the simulation parameters for the hybrid MG system. The Simulink model of the MG under consideration includes a 1.1 kV solar PV system with a solar array comprising 20,000 module strings and 200,000 parallel strings.

Table 1: Simulation parameters of proposed system

PV System	Irradiance	1000 W/m ²
	I _{sc}	7.35 A
	V _{oc}	0.6 V
	Temperature	45 ⁰ C
Wind Turbine	Generator Power	2 kVA
	Generator Speed	3500 rpm

Battery System	Pitch Angle	15 ⁰
	Load	1000 kW
	Battery Voltage	400 V
	Battery Capacity	500 Ah
	Initial SOC	100 %
	Discharge Rate	6.6: 13: 32 A

The key components of the envisioned model include a wind turbine, a PV system, an MPPT-based boost converter, a battery, and controllers for diverse PWM generation. Fig. 3 showcases the Simulink model of MG system.

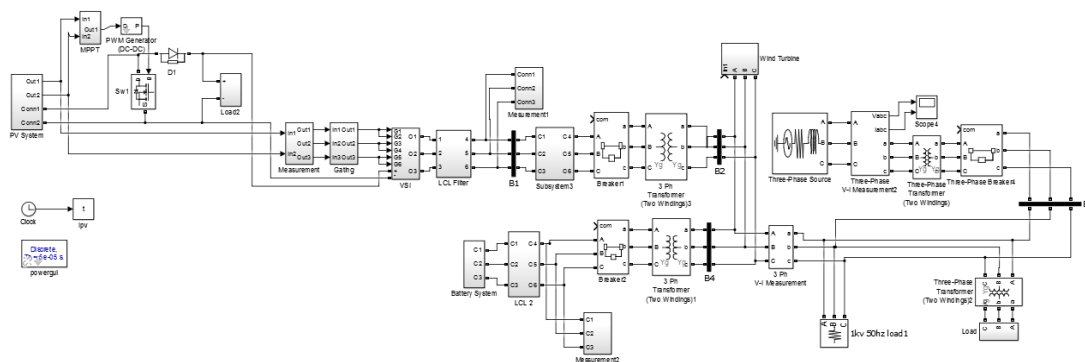


Fig. 3: Simulink layout of MG system.

The simulated voltage and current outputs are directed to a shared electrical bus or node. This common bus serves as a central point where the electrical outputs from different PV modules or arrays are integrated. The simulated waveforms depicted in Fig. 4 offer a comprehensive view of how the voltage and current fluctuate over time and under diverse operational scenarios. Analyzing these waveforms is crucial for assessing the performance, stability, and compatibility of the PV system with other components within the broader electrical framework.

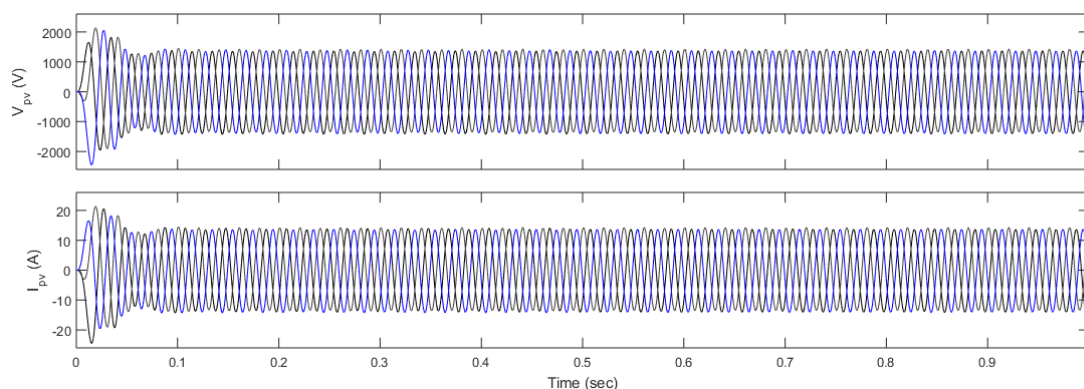


Fig. 4: 3-Phase Voltage and Current of PV Inverter.

Six batteries, each with an input voltage of 400 volts and 500 amperes, are arranged in series and collectively supplied as input to the inverters. The resulting AC voltage and current profiles are illustrated in Fig. 5. This configuration of connecting batteries in series allows for the cumulative voltage to be additive, providing a total input voltage of 2400 volts (400 volts multiplied by 6 batteries). Simultaneously, the current remains constant at 500 amperes as it flows through the series-connected batteries.

The corresponding AC voltage and current waveforms showcase the electrical behavior of the system as it undergoes inversion, transforming the DC input from the batteries into AC. Analyzing these waveforms provides valuable insights into the performance and characteristics of the inverter system operating with the specified battery setup.

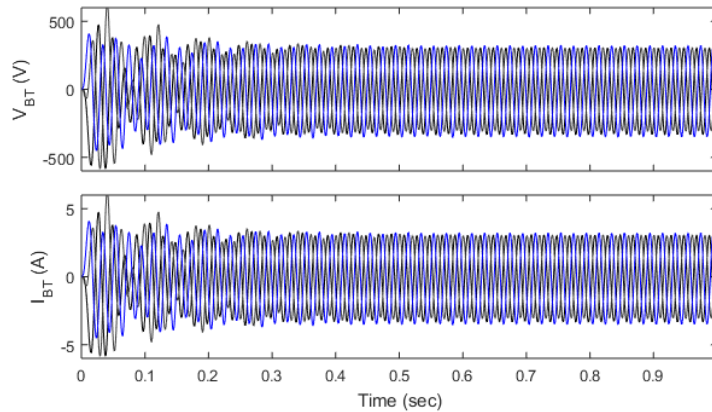


Fig. 5: AC Voltage and Current of Battery Inverter System

The AC output generated from the WT operating at a wind speed of 12 m/s is acquired and visually represented in Fig. 6. This figure illustrates the electrical output in terms of AC produced by the wind turbine under the specified wind speed condition. The generated AC output is indicative of the efficiency and performance of the wind turbine in harnessing wind energy and converting it into electrical power. Analyzing the waveform and characteristics presented in Fig. 6 allows for a comprehensive understanding of how the wind turbine responds to the given wind speed, offering valuable insights into its operational behavior and effectiveness in converting wind kinetic energy into usable electrical power.

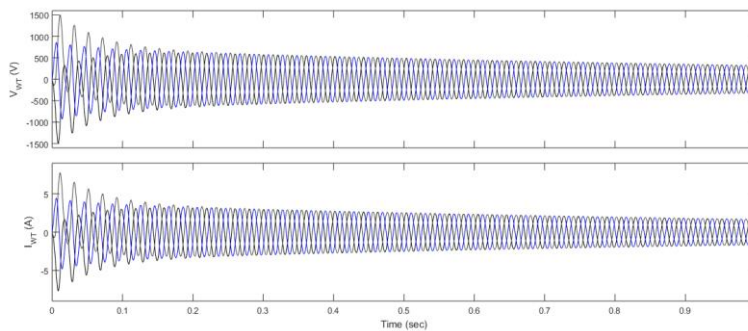


Fig. 6: 3-Phase Voltage and Current of Wind Turbine

The voltage and current of the PV system undergo control through a MPPT boost converter, after which the output of the MPPT is directed into the inverter. The analysis of the DC output voltage from the MPPT boost converter is illustrated in Fig. 7. Remarkably, the graph indicates that the boost converter effectively maintains a consistent output voltage throughout the simulated period. Moreover, it ensures a 100% SOC, emphasizing the converter's capability to optimize the PV system's performance and sustain a fully charged state during the simulation. This outcome underscores the reliability and efficiency of the MPPT boost converter in regulating the DC output voltage, a critical aspect in enhancing the overall performance and energy harvesting capability of the PV system.

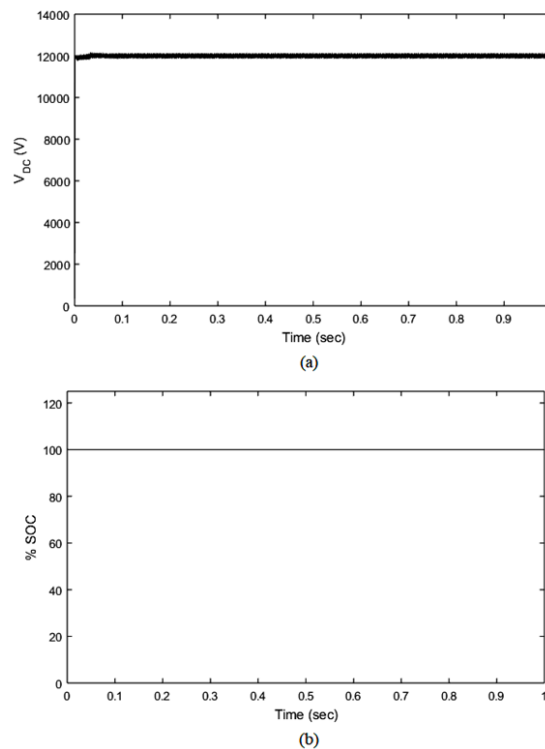


Fig.7: Output Analysis (a) MPPT output, (b) SOC of Batteries

Fig. 8 showcases the grid voltage and current, characterized by a consistent amplitude and balanced phase. In this depiction, generators are interconnected at 11 kV, generating flawless sinusoidal AC voltage tailored for the load under grid-connected mode. The constancy of amplitude and balanced phase observed in the graph underscores the reliability and stability of the suggested method. The synchronous and harmonic-free behavior of the generated AC voltage showcase the maintenance of desired electrical characteristics during grid connection. This assurance of a stable and well-regulated grid connection mode reinforces the credibility and practical viability of the employed methodology.

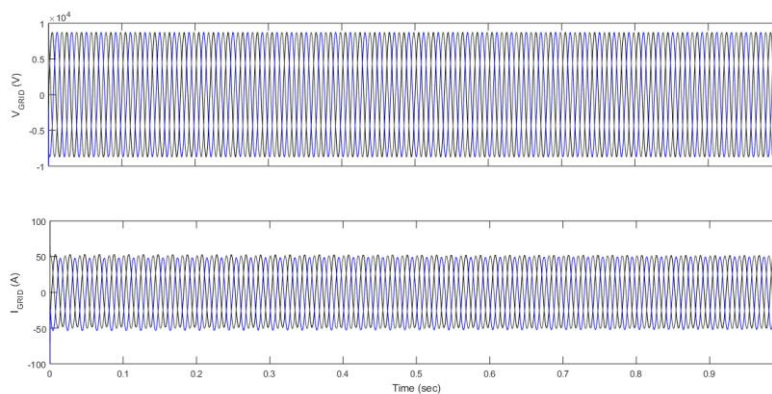


Fig. 8: AC Voltage and Current of Grid System.

Proposed system integrates the PV system, WT system, and Battery system, showcasing various parameters. Table 2 provides a comprehensive overview of the acquired values derived from the presented results of the proposed hybrid system. The table serves as a valuable reference, presenting the detailed performance metrics and characteristics of each component within the hybrid system. The inclusion of real power and reactive power values elucidates the active and reactive energy contributions, while THD values offer insights into the harmonic content of the system. Voltage and current readings further contribute to a holistic understanding of proposed hybrid system's operational effectiveness and efficiency.

Table 2: Performance Comparison

Parameter	PV System		Wind Turbine		Battery System	
	Firefly-PSO	APSO	Firefly-PSO	APSO	Firefly-PSO	APSO
Real Power (W)	6×10^4	8×10^4	2×10^4	4×10^4	1500	4500
Reactive Power (kVAR)	3×10^4	6×10^4	2×10^4	4×10^4	2.5×10^{10}	4×10^{10}
THD (%)	5	5.5	3.5	4	7	8
Voltage(V)	1000	1500	500	1000	200	300
Current(A)	15	15	3	3	3	3

5. CONCLUSION

In the course of this research, the primary focus has been on the meticulous design and implementation of a grid-connected AC microgrid, incorporating essential components such as solar PV, battery, and a wind turbine. To optimize the system's performance, a control mechanism was introduced utilizing an optimization algorithm. Specifically, the conventional droop control system, responsible for maintaining a consistent load voltage, underwent enhancement through the incorporation of a hybrid APSO algorithm. The noteworthy aspect of this study lies in the comparative analysis of the APSO algorithm against the existing approach, which combines PSO with the initial optimization process. The results highlight the superior performance of the APSO algorithm in regulating crucial electrical parameters such as real power, reactive power, Total THD, and voltage and current outputs. This optimized control strategy exhibits enhanced precision and efficiency when compared to the previously employed PSO with the firefly algorithm, signifying its potential to significantly improve the overall stability and effectiveness of the microgrid system. The findings underscore the importance of incorporating advanced optimization techniques for achieving superior control and operational outcomes in complex energy systems like AC microgrids.

REFERENCES

- [1] B. U. Kansara and B. R. Parekh, "Modelling and simulation of distributed generation system using HOMER software," *International Conference on Recent Advancements in Electrical, Electronics and Control Engineering*, 2011, 371–376.
- [2] M. S. Mahmood, S. A. Hussain and M. A. Abido, "Modeling and control of microgrid: An overview Author links open overlay panel," *Journal of Franklin Institute*, vol. 351, no. 5, pp. 2822-2859, 2014.
- [3] V. O. Okinda and N. A. Odero, "Modelling, Simulation and Optimal Sizing of a Hybrid Wind, Solar PV Power System in Northern Kenya," *International Journal of Renewable Energy Research*, vol. 6, no. 4, 2016.
- [4] H. Lan, S. Wen, Y. YiHong, and D. C. Yu, "Optimal sizing of hybrid PV/diesel/battery in ship power system," *Applied Energy*, vol. 158, pp. 26-34, 2015.
- [5] D. Das, G. Gurralla and U. J. Shenoy, "Transition between grid-connected mode and islanded mode in VSI-fed microgrids," *Springer Sadhana*, vol. 42, no. 8, pp. 1239-1250, 2017.
- [6] R. Tidjani, F. S. Hamadi, A. Chandra, A. Pillay and A. Ndtoungou, "Optimization of standalone microgrid considering active damping technique and smart power management using fuzzy logic supervisor," *IEEE Transactions on Smart Grid*, vol. 8, no. 1, pp. 475-484, 2017.
- [7] W. Jewell and R. R. Kumar, "The effects of moving clouds on electric utilities with dispersed photovoltaic generation," *IEEE Transaction on Power Apparatus and System*, vol. 7, no. 12, 2017, 2237–2248.
- [8] F. A. Jiang, W. F. Jiang and A. Wong, "Study on the performance of different types of pv modules in Singapore," *International Power Engineering Conference*, Singapore, 2015, 1104–1110.
- [9] K. Y. Lau, M. M. Yousof, S. M. Arshad, M. Anwar and A. M. Yatim, "Performance analysis of hybrid photovoltaic/diesel energy system under Malaysian conditions," *Energy*, vol. 35, no. 8, pp. 3245-3255, 2010.

- [10] H. Kanchev, D. Lu and F. Colas, "Energy management and operational planning of a micro –grid with a PV based active generator for smart grid application," *IEEE Transaction on Industrial Electronics*, vol. 58, no. 10, pp. 4583-4592, 2021.
- [11] C. Jian, C. Yanbo and Z. Jijie, "Optimal Configuration and Analysis of Isolated Renewable Power Systems," in *4th International Conference on Power Electronics Systems and Applications, Hongkong*, 2018, 108-120.
- [12] V. Bala Raju and K. Vimalakumar, "Application of Advanced Inverters in Interconnection of Renewable Energy Sources to the Electrical Grid at the Distribution system," in *IJERA; Advances in Energy and Power Control Engineering*, 2012, 832–837.
- [13] R. Al Badwawi, W. Issa, M. Abusara and M. Tapas, "Supervisory Control for Power Management of an Islanded AC Microgrid Using Frequency Signaling-Based Fuzzy Logic Controller," in *IEEE Transactions on Sustainable Energy*, 2018, vol. 58, no. 10, pp. 583-592.
- [14] G. Gust, T. Brandt, S. Mashayekh, M. Heleno, and D. Neumann, (2021). Strategies for microgrid operation under real-world conditions. *European Journal of Operational Research*, 292(1), 339-352.
- [15] J. Yang, and C. Su, "Robust optimization of microgrid based on renewable distributed power generation and load demand uncertainty," *Energy*, 223, 120-134, 021.
- [16] L. Yin, K. Kim, F. Tehrani, F. Lin, M. Lin, and J. Wang, J. "A self-sustainable wearable multi-modular E-textile bioenergy microgrid system," *Nature Communications*, 12(1), 1542-1547, 2021.

Email: fa.ahmad@paaet.edu.kw